Expression patterns of RelA and c-mip are associated with different glomerular diseases following anti-VEGF therapy.

Hassan Izzedine, Melanie Mangier, Virginie Ory, Shao-Yu Zhang, Kelhia
Sendeyo, Vincent Audard, Christine Péchoux, Jean C. Soria, Christophe
Massard, Rastilav Bahleda, et al.

C-mip and NF-kB define two distinct renal syndromes associated with VEGF-targeted therapy

SCHOLARONE™
Manuscripts

1
2
3
4
5
6
7
8
9
10
11
12
13
14
15
16
17
18
19
20
21
22
23
24
25
26
27
28
29
30
31
32
33
34
35
36
37
38
39
40
41
42
43
44
45
46
47
48
49
50
51
52
53
54
55
56
57
58
59
60

C-mip and NF-kB define two distinct renal syndromes associated with VEGF-targeted therapy

Hassan Izzedine[1*], Melanie Mangier[2,3*], Virginie Ory[2,3], Shao-Yu Zhang[2,3], Kelhia Sendeyo[2,3], Vincent Audard[2,3,7], C. Péchoux[4], Jean Charles Soria[5], Christophe Massard[5], Rastilav Bahleda[5], Edward Bourry[1], David Khayat[6], Alain Baumelou[1], Philippe Lang[2,3,7], Mario Ollero[2,3], Andre Pawlak[2,3], Djillali Sahali[2,3,7].

Departments of [1]Nephrology, [5,6]Medical Oncology,

[1,5]Pitie-Salpetriere Hospital, Paris, France

[5]Institut Gustave Roussy, VilleJuif, France

[2]INSERM, U 955, Equipe 21, F-94010, Créteil, France.

[3]Université Paris-Est Creteil Val-de-Marne, F-94010, Créteil, France.

[4]INRA, UR1196 Génomique et Physiologie de la Lactation, plateforme MIMA2, F-78352, Jouy-en-Josas Cedex, France

[7]AP-HP, Groupe hospitalier Henri Mondor-Albert Chenevier, Service de Néphrologie, F-94010, Créteil, France.

* HI and MM contributed equally to this work

Corresponding authors:

Hassane Izzedine and Djillali Sahali.

Dr Hassane Izzedine, Service de Néphrologie, APHP, Université Pierre and Marie Curie, Paris VI, Groupe Hospitalier Pitié-Salpêtrière, Paris 75013, France. hassan.izzedine@psl.aphp.fr

Dr Djillali Sahali, Service de Néphrologie, APHP, Université Paris-Est Créteil Val-de-Marne, UMRS 955, Equipe 21, Groupe hospitalier Henri Mondor-Albert Chenevier, Créteil, F-94010 France. dil.sahali@inserm.fr

Abstract

Renal toxicity constitutes a dose-limiting side effect of anticancer therapies targeting the vascular endothelial growth factor (VEGF). We studied twenty-nine patients having followed this kind of treatment. Eight of them developed minimal change nephropathy (MCN)/focal segmental glomerulopathy (FSG)-like lesions and thirteen thrombotic microangiopathy (TMA). MCN/FSG-like lesions developed mainly under receptor tyrosine kinase inhibitor (RTKI), whereas TMA complicated anti-VEGF therapy. Patients with TMA had no mutations in factors H, I, or membrane cofactor protein of the complement alternative pathway, while plasma ADAMTS13 activity persisted and anti-ADAMTS13 antibodies were undetectable. Glomerular VEGF expression was decreased in MCN/FSG and undetectable in TMA. Glomeruli of TMA displayed a high abundance of RelA in endothelial cells and in the podocytes nuclei, but c-mip was not detected. Conversely, MCN/FSG-like lesions exhibited a high abundance of c-mip, whereas RelA was scarcely detected. RelA binds in vivo to *c-mip* promoter and prevents its transcriptional activation, whereas knockdown of RelA releases the activation of *c-mip*. The RTKI sorafenib inhibits RelA activity and promotes c-mip expression. These observations suggest that c-mip and RelA define two distinct renal damages associated with VEGF-targeted therapies.

Introduction

In renal glomeruli, podocytes express vascular endothelial growth factor (VEGF), whereas VEGF receptor tyrosine kinases are expressed by both podocytes and glomerular endothelial cells.[1] The biological functions of VEGF are mediated by its binding to one of the VEGF receptor tyrosine kinases (RTKs), which include VEGFR-1 (Flt-1), VEGFR-2 (KDR/Flk-1), and VEGFR-3 (Flt-4). The VEGF family comprises seven members, VEGF-A, -B, -C, -D, -E, and placenta growth factor 1 and 2 (PlGF1 and PlGF2). VEGF-A (also referred to as VEGF) binds to VEGFR-1 and -2, while VEGF-C and -D bind to VEGFR-2 and VEGFR-3. VEGFR2 expression has been reported in cultured podocytes.[2] Structurally, RTKs consist of an extracellular ligand-binding domain, a transmembrane region, and an intracellular, kinase domain that mediates downstream signal transduction. Upon binding to their ligand, RTKs dimerize and are phosphorylated on their kinase domain, leading to the recruitment of adaptor proteins that trigger intracellular signaling cascades important for processes such as cell proliferation and survival, migration and metabolism.[3] Dysregulation of RTK signaling by mutation or by ectopic receptor or ligand overproduction has been implicated in several aspects of tumor progression, including cell proliferation, survival, angiogenesis and tumor dissemination.[4]

VEGFR-2 is the predominant receptor in angiogenic signaling.[5, 6] VEGF is upregulated in response to hypoxia, oncogenes, or cytokines, and its expression is associated with poor prognosis in several types of cancer.[7, 8]

Experimental, preclinical and clinical studies have identified angiogenesis as a key process in the progression of most solid tumors. Thus, inhibition of VEGF and PDGF signaling is predicted to lead to anti-angiogenic effects and prevent the progression of tumors.[9, 10] Therapeutic approaches targeting the VEGF ligand or RTK inhibitors (RTKIs) have recently

been developed. Several antagonists of VEGF signaling are being tested in clinical trials, including bevacizumab (anti-VEGF monoclonal antibody), and RTK inhibitors (RTKI) such as sunitinib, imatinib and sorafenib.[11] Although RTKI are widely used as inhibitors of VEGFRs, they interfere with the activity of other growth factors, among them PDGFRs, stem cell factor receptor (c-kit), FMS-like tyrosine kinase-3 (Flt-3), b-raf and Bcl-Abl. Thus, they are commonly named as multitargeted RTKI and widely used in medical oncology practice. However, renal complications constitute a dose-limiting side effect of RTKI and anti-VEGF therapies.

We report here on a series of twenty-nine patients treated with anti-VEGF and RTKI who experienced proteinuria, hypertension and/or renal insufficiency. Immunomorphological and molecular studies suggest that RelA and c-mip define two separate glomerular damages associated with anti-angiogenic drugs.

Results

Clinical characteristics of patients with renal diseases

Baseline patient characteristics are summarized in Table 1. All patients were referred to a nephrology department because of discovery of proteinuria and/or increased serum creatinine following anti-VEGF initiating treatment. Sixteen patients had renal cell carcinoma and received 50 mg of sunitinib daily (n=11), 400 mg of sorafenib (n=3) or 5 mg axitinib (n=1) twice daily, or bevacizumab (10 mg/kg/dose) twice monthly (n=2). Thirteen other patients received VEGF Trap (4 to 6 mg/kg/dose) every three weeks (for ovarian, adrenal, breast, prostate, esophageal and rectal cancers), or bevacizumab 10 mg/kg/dose twice monthly (for lung, uterine and colorectal cancers). At the time of kidney biopsy, 20 patients (68,9%) presented with hypertension requiring antihypertensive treatment and 14 (48,3%) with renal failure defined by a creatinine clearance rate below 60 ml/min/1.73m^2. Kidney biopsy was performed 2 to 12 weeks after the start of anti-VEGF treatment. Average number of glomeruli was 18.2 (range: 9-50). The principal pathological findings were TMA (n=13), MCN/FSG-like syndromes (n=8), acute tubular necrosis (n=3), and one case of each of the following lesions: membranous nephropathy, IgA nephropathy, ANCA negative pauciimmune crescentic glomerulonephritis, diabetic nephropathy and acute interstitial nephritis. Overlapping features of nephroangiosclerosis (7 patients) accompanied the other pathological findings. Fourteen patients (56%) died during the study due to cancer progression. Due to the expected limited survival, managing oncologists were reluctant to repeat the urinary investigations.

MCN/FSG like damages

Eight patients with a previous nephrectomy for metastatic renal cell carcinoma (mRCC) and/or interferon alpha therapy exhibited MCN/FSG-like lesions, defined by nephrotic

proteinuria (with or without hypoalbuminemia), while light microscopy examination showed either normal glomeruli or FSGS lesions. These patients had received sunitinib (5 patients), sorafinib (2 patient) and Axitinib (1 patient). The mean interval between initiation of RTKI therapy and onset of proteinuria was 65 ± 50.5 days (range 14–180). All patients displayed heavy proteinuria but only two exhibited hypertension and acute renal failure. Anti-VEGF therapy was discontinued in all patients, and symptomatic treatments such as angiotensin converting enzyme inhibitors or angiotensin-2 receptor antagonists were started. Six patients died shortly thereafter due to cancer progression.

Renal thrombotic microangiopathy

Thirteen patients presented with renal TMA. Platinium derivatives (n=3), gemcitabine (n=1) or radiotherapy (n=1) were administered prior to anti-VEGF agents. No clinical or biological signs of TMA were observed during gemcitabine treatment, which was given six months before the introduction of anti-VEGF medications. The mean interval between initiation of anti-VEGF therapy and the onset of TMA was 5.75 ± 3.6 months (range 2–12). Anti-VEGF agents included bevacizumab (between 2 and 24 doses in six patients), VEGF Trap (after 2, 3, 4, 8, and 9 cycles in five patients, respectively) and sunitinib (after 2 cycles in two patients). All patients showed significant proteinuria (including eight with nephrotic syndrome), while eight had hypertension. Two patients developed acute renal failure and six displayed microhematuria. Fifty percent of patients who developed TMA displayed haematological manifestations. Anemia and thrombocytopenia were absent in 3 patients, while haptoglobin was normal in 7 patients. Schistocytes were absent in 4 patients. Renal biopsies revealed TMA in all patients, characterized by glomerular capillary thrombosis associated with mesangiolysis and double contours. All patients exhibited normal complement proteins. No constitutional abnormalities or heterozygous missense mutations were found in Factors H, I,

or MCP, the 3 major regulatory proteins of the complement alternative pathway (CAP).

Plasma ADAMTS13 activity was above 20 percent. Acquired or constitutive anti-

ADAMTS13 antibodies were undetectable. Different symptomatic treatments were tried,

including plasmapheresis and fresh frozen plasma (7 patients), as well as steroid and

antihypertensive drugs. Renal and hematological symptoms were improved one to six months

after the discontinuation of anti-VEGF agents. Five patients died because to cancer

progression. One patient switched to another anti-VEGF agent (from VEGF Trap to

bevacizumab) and displayed an absence of proteinuria and stable renal function two years

later. Another patient continued bevacizumab in association with antihypertensive drugs for 8

months despite persistent proteinuria but renal function remained stable.

Differential expression of VEGF, HIF1α, c-mip, RelA and Tie2 in glomeruli with TMA and MCN/FSG-like lesions

The relative abundance of VEGF was reduced in podocytes from patients with MCN/FSG

when compared to control kidney tissues and undetectable in TMA (Figure 1a), as previously

reported.[12]

Quantification of the relative abundance of c-mip, RelA, HIF1α and Tie2, as well as their

expression pattern were analyzed in all glomeruli of MCN/FSGS or TMA biopsies and

compared to idiopathic forms (iMCNS, iFSGS and iTMA) (Figure 1 and supplementary

Figure S1). For quantification, five biopsies corresponding to each pathological condition

were assessed and the data are depicted in Figure 1f. The relative abundance of c-mip was

greatly increased in MCN/FSG-like lesions but no significant difference was observed with

idiopathic MCNS and FSGS diseases, whereas it was scarcely or not detected in TMA or in

control human kidneys (Figure 1b and f). Hypoxia-inducible factor 1α (HIF-1α) is an

oxygen-sensitive transcription factor that is recruited in response to oxygen deprivation. We

reasoned that in TMA ischemic conditions prevail and would result in a loss of oxygen delivery to tissues, leading to HIF-1α activation. In biopsies with MCN/FSG-like lesions, HIF1α expression was increased as compared with control human kidney, but higher abundance was observed in TMA glomeruli without significant difference between idiopathic- and VEGF forms (Figure 1c and f). Idiopathic MCNS and FSGS are considered as non-inflammatory glomerular diseases.[13] We investigated whether, unlike the idiopathic forms, inflammation may occur in MCN/FSG-like syndrome. Therefore, we analyzed the expression of RelA, a master NF-κB transcription factor, which controls many inflammatory genes.[14] The relative abundance of RelA was significantly higher in TMA than in control human kidneys, whereas it was scarcely detected in MCN/FSG-like lesions (Figure 1d and f). Subtle differences in RelA abundance and distribution were observed between anti-VEGF-induced TMA and the idiopathic forms: RelA was uniformly increased in idiopathic TMA glomeruli, but higher abundance was observed in anti-VEGF therapy-related TMA glomeruli (Figure 1f) with a more restricted distribution to some capillary loops (Figure 1d and supplementary Figure S1). On the other hand, RelA abundance was clearly reduced in idiopathic MCNS and FSGS, as well as in MCN/FSG-like lesions, as compared with control human kidneys, without significant difference between idiopathic forms and anti-VEGF-related lesions (Figure 1f). The relative abundance of Tie2 was significantly increased after anti-VEGF or RTKI therapies (Figure 1e and f).

Confocal microscopy analysis showed that nephrin expression was significantly reduced and exhibited a granular pattern in MCN/FSG relatively to control human kidneys (Figure 2). In contrast, nephrin displayed variable expression and an irregular pattern in TMA glomeruli consisting of a lack of detection in some areas and preservation in others. In control human kidneys, RelA was located on the external side of the specific endothelial cell marker Tie2

showing no colocalization, which suggests that RelA was only expressed in podocytes (Figure 3). The relative abundance of RelA was dramatically increased in TMA glomeruli, not only in podocytes but also in endothelial cells, as shown by double labelling RelA/nephrin (Figure 2) and RelA/Tie2 (Figure 3), respectively. Tie2 immunostaining showed a slight increase in MCN/FSG biopsies compared to control kidneys. Tie2 expression was strongly increased in TMA with a diffuse, irregular pattern within the capillary loops (Figure 3). These results suggest that in MCN/FSG-like syndromes associated with RTKI therapy, glomerular lesions affect podocytes almost exclusively, whereas in TMA, alterations mainly affect endothelial cells and podocyte injury may be a secondary event. Significant changes were also observed in small arterioles in TMA biopsies, where endothelial cells were swollen and exhibited higher abundance of RelA (Figure 4), when compared to endothelial cells from normal arterioles. Moreover, arteriolar walls were infiltrated by pericytes that exhibited high amount of RelA. These changes were not observed in the control human kidneys.

We studied ultrastructural alterations in glomeruli of patients with bevacizumab-induced TMA and in control kidneys (n=3 each). Transmission electron microscopy analysis showed major alterations in TMA glomeruli including duplication of GBM, loss of fenestrations, detachment of endothelial cells from original basement membrane, interposition of cells and marked effacement of visceral epithelial cell foot processes in some areas. Some podocytes exhibited cytoplasm vacuolization as well as endoplasmic reticulum enlargement and mitochondrial swelling, suggesting an underlying apoptotic process (Figure 5a). To provide accurate determination of RelA increase in bevacizumab-induced TMA, we performed immunogold labeling and quantified the number of RelA gold particles in podocytes and in endothelial glomerular cells. In TMA kidney biopsies, the number of RelA gold particles was strongly increased in nuclear podocytes, as well as in endothelial glomerular cells as

compared with control kidney (p<0.001), while no significant difference was detected in the

cytoplasm of podocytes (Figure 5b and c).

NF-κB binds to c-mip promoter and inhibits its transcriptional activity

Given the increased abundance of RelA in TMA contrasting with the virtual absence of c-

mip, we hypothesized that *c-mip* expression was repressed at the transcriptional level by NF-

κB. NF-κB-heterodimers bind to 10 bp κB DNA sites that exhibit the consensus sequence (5'-

GGGRNWYYCC-3'), which comprises a constant core and a number of variable nucleotides

(R: A or G; N: any nucleotide; W: A or T; Y: C or T). The sequence identified on the human

c-mip promoter (c-mip-κB, 5'-GGGGCTGCCC-3') at position -199 to -214 (+1 corresponds

to the transcriptional initiation site) fulfils these criteria (Figure 6a**).** The mouse κB response

element (κB-RE) is identical to that of humans, except for the substitution of the T-nucleotide

by a C-nucleotide (5'-GGGGCCGCCC-3'). To assess whether NF-κB binds to this sequence

in vivo, we performed chromatin immunoprecipitation using mouse podocytes. The short

region flanking the κB-RE was precipitated by the anti-RelA antibody, but not by the rabbit

IgG control (Figure 6b**)**. Incubation of nuclear extracts from HEK cells overexpressing RelA

with the radiolabeled c-mip κB-RE oligonucleotide produced only one specific band shift in

EMSA (Figure 6c**)**. The DNA binding shift appeared to be specific since it was abolished by

co-incubation with a mutated probe and shifted upwards in the presence of the anti-RelA

antibody. In contrast, the lower band shifts observed with the mutated c-mip-κB seemed to be

non-specific, as they were not altered by the preincubation of nuclear extracts with the anti-

RelA antibody. This result led us to study the effects of NF-κB on the transcriptional

activation of *c-mip*. The 877 bp full-length sequence containing the entire *c-mip* proximal

promoter was ligated upstream of the luciferase gene and cotransfected with NF-kB p50,

p65/RelA or both, as well as with the empty vector. Protein lysates were prepared 24 hours

following transfection. Luciferase activity driven by the *c-mip* promoter was strongly reduced in the presence of RelA (Figure 6d). Interestingly, overexpression of p50 alone did not inhibit the transcriptional activity of *c-mip* promoter. Moreover, cotransfection of RelA with p50 significantly reduced the inhibition of luciferase activity induced by RelA alone. These results suggest that RelA binds to the *c-mip* promoter and exerts a powerful inhibitory effect on *c-mip* transcription. A strong argument supporting this hypothesis came from the study of wild-type and RelA-deficient mouse embryonic fibroblasts (MEF). Figure 7 shows that c-mip was dramatically increased in RelA-deficient MEF, in the absence of any treatment, whereas it was barely detected in wild-type MEF.

Sorafenib induces overexpression of c-mip in vivo and in vitro

We investigated whether overproduction of c-mip in MCN/FSG-like lesions is a secondary molecular event or a direct effect of RTKI. At first, we tested whether sorafenib affects c-mip expression in wild-type and RelA-deficient MEF. The abundance of c-mip is remarkably higher in RelA-deficient MEF as compared with wild-type MEF (Figure 8a). However, preincubation of cells with sorafenib increased the basal amount of c-mip, both in wild-type and RelA-deficient MEF. We then treated a podocyte cell line with sorafenib and analyzed *c-mip* expression by quantitative PCR. The abundance of transcript was significantly increased in podocytes treated with sorafenib when compared with those incubated with the vehicle only (ethanol) (Figure 8b). Because VEGF receptor is also expressed by lymphocytes, we tested whether sorafenib affects c-mip expression in these immune cells. We purified lymphocytes from normal donors by cell gradient density and incubated them with the same concentration of sorafenib. Interestingly, c-mip was also increased in normal lymphocytes, suggesting that the induction of c-mip by sorafenib was not restricted to podocytes (Figure 8c).

Sorafenib inhibits RelA activation

In resting cells, RelA is mostly sequestered in the cytoplasm compartment by its inhibitor IκBα. Stimulation of cells by NF-κB inducers such as cytokines induces phosphorylation of IκBα at serine (Ser) residues 32-36, followed by its ubiquination and proteasome degradation. RelA released from its inhibitor is phosphorylated and moves into the nucleus where it promotes transcriptional activation of target genes.[15] Phosphorylation of RelA at serine 276 plays a crucial role in NF-κB transcriptional activity. [16] Inhibition of RelA phosphorylation at serine 276 has been implicated in the transactivation inhibition of NF-κB–dependent genes.[17] Because RelA inhibits transcriptional activation of c-mip, we looked whether c-mip upregulation in MCN/FSG results from direct inhibition of RelA activity by RTKI therapy. Therefore, we treated the podocyte cell line with sorafenib and analyzed the activation status of RelA and its subcellular localization, as well as the stability of IκBα. In the absence of sorafenib, phospho-ser[32-36] IκBα was detected, along with phospho-ser[276] RelA, suggesting that NF-κB is constitutively activated in the podocytes (Figure 9a). Conversely, Sorafenib blocked RelA phosphorylation, whereas IκBα phosphorylation was significantly reduced, these effects were sustained for at least 48 hours. Immunoblotting of cytoplasm and nuclear podocyte extracts showed that Sorafenib induces accumulation of RelA in the cytoplasm, while very low abundance of RelA was detected in nuclear extracts (Figure 9b). In addition immunoprecipitation experiments showed that RelA was mostly sequestered with IκBα in podocytes incubated with Sorafenib (Figure 9c). Confocal microscopy analysis showed that RelA was diffusely expressed in both cytoplasm and nuclear compartment in untreated cells, whereas its expression was mostly restricted to cytoplasm in sorafenib-treated cells (Figure 9d). These results suggest that sorafenib inhibits NF-κB activity and indirectly promotes *c-mip* transcriptional activation.

1
2
3
4
5
6
7
8
9
10
11
12
13
14
15
16
17
18
19
20
21
22
23
24
25
26
27
28
29
30
31
32
33
34
35
36
37
38
39
40
41
42
43
44
45
46
47
48
49
50
51
52
53
54
55
56
57
58
59
60

Discussion

Anti-VEGF therapy leads to various glomerular injuries, including MCN/FSG- and TMA-like syndromes. In our group of patients, we show for the first time that MCN/FSG lesions, which mostly observed following RTKI therapy, are associated with high abundance of c-mip. In contrast, in TMA resulting from anti-VEGF therapy, c-mip is not detected, while RelA is produced at high levels by podocytes and glomerular endothelial cells. We provide evidence that RelA binds to *c-mip* promoter i*n vivo* and represses its transcription, while knock down of RelA releases this inhibition. These results may account for the non-expression of c-mip in the podocytes of patients with TMA. Conversely, inhibition of RelA activity promotes c-mip expression.

The association between occurrence of proteinuria and the inhibition of VEGF signaling is now established. [18] Despite the fact that our patients with MCN/FSG were older (mean, 71.5 yrs) as compared with TMA group (mean, 69.5 yrs) and had previously received interferon-α, proteinuria was negative before the introduction of RTKI therapy. Furthermore, patients did not receive any bisphosphonate, known to be toxic for podocytes. Finally, the development of proteinuria in all patients closely paralleled the administration of RTKI.

TMA has been reported to be associated with several anti-VEGF agents such as bevacizumab,[19, 20] VEGF Trap [21] and sunitinib,[20, 22] suggesting a class adverse effect. In our series, TMA was observed in 11/15 patients following bevacizumab and VEGF Trap therapies. These lesions were characterized by high abundance of RelA in endothelial cells and in podocytes.

The podocyte-specific deletion of VEGF in adult transgenic mice induces TMA.[12] In this model, thrombotic glomerular injury and heavy proteinuria precede the development of

hypertension, making hypertension unlikely to be the cause of proteinuria. In our patients presenting with TMA, glomeruli exhibited high abundance of RelA, suggesting that abnormal cell signaling induced by anti-VEGF treatment led to the recruitment of NF-κB and activation of target genes at the sites of injury. Reduced endothelial NF-κB activity decreases albuminuria independently of its effects on blood pressure in transgenic mice with endothelial cell–restricted NF-κB super-repressor overexpression.[23], [24] The increase in intrarenal angiotensin II induced by proteinuria depends on NF-κB activation. By inhibiting not only the induction of proinflammatory cytokines but also the activation of the intrarenal renin-angiotensin system, the inhibition of renal NF-κB activation may be therapeutically useful as a means of retarding the development and progression of renal damage associated with persistent proteinuria.[25] Our findings suggest that the inhibition of NF-κB could have a beneficial effect in the management of TMA associated with anti-VEGF therapy.

Several pathophysiological mechanisms have been put forward for the occurrence of MCN/FSG-like lesions in patients undergoing RTKI therapy.[18] The high incidence of RCC in our cohort (60%) suggests a possible role for the adaptive hyperfiltration response to nephrectomy, as reported in the literature.[26] However, in our patients proteinuria was still absent at least one year after nephrectomy and developed rapidly only after initiation of anti-VEGF therapy, ruling out a potential close link between unilateral nephrectomy and proteinuria, although we cannot exclude the possibility that the former may promote RTKI-induced podocyte injury.

Several signaling molecules have been shown to interact with VEGFR2 including the regulatory p85 subunit of PI3-kinase,[27] Fyn and Nck.[28] VEGFR-2 is rapidly phosphorylated in response to VEGF and leads to the recruitment of Fyn, which then initiates a cascade of phosphorylation events involving Nck, PAK-2 and N-WASP, resulting in actin polymerization and actin stress-fiber formation.[28], [29]

VEGFR2 expression in podocytes is still debated. Compelling evidence suggests that VEGFR2 is expressed in a differentiated podocyte cell line,[2] as well as in mouse podocytes.[30] Moreover, VEGFR2 interacts *in vitro* and *in vivo* with nephrin, a specific podocyte marker.[31] Although these data suggest that podocytes possess a functional autocrine VEGF-VEGFR2 system, another group has failed to detect VEGFR2 in podocytes *in vivo*.[32] In addition, this group has shown that knockdown of VEGFR2 in podocytes has no effect on glomerular development and function.

The data presented here strongly suggest that RelA is a repressor of c-mip. Because RelA is constitutively expressed in podocytes, the lack of c-mip detection in control glomeruli is not unexpected. Conversely, inhibition of NF-κB activity by RTKI therapy, also reported by other authors,[33] leads to c-mip overexpression and induces human podocyte disease with nephrotic proteinuria, reminiscent of the transgenic c-mip mouse model.

We have recently reported that c-mip abundance increases in the podocytes of patients with acquired idiopathic nephrotic syndromes, including primary MCNS and FSGS, in which podocytes are the main target of injury.[34] Transgenic mice that overexpress c-mip in podocytes develop heavy proteinuria without inflammatory lesions or cell infiltration. We have shown that c-mip turns off podocyte signaling by preventing the interaction of nephrin with Fyn, thereby decreasing nephrin phosphorylation *in vitro* and *in vivo*.[34] We have also shown that c-mip inhibits the interaction between Nck and nephrin and between Fyn and N-WASP, potentially accounting for cytoskeletal disorganization and the effacement of foot processes.[34] Moreover, the intravenous injection of a small interfering RNA (siRNA) targeting c-mip prevents lipopolysaccharide-induced proteinuria in mice.[34] These results suggest that c-mip plays a crucial role in podocyte dysfunction leading to proteinuria.

Renal TMA is a serious complication that usually leads to drug withdrawal.[12, 19-22] The physician must be aware of these rare complications, institute surveillance for renal

dysfunction and thoroughly investigate patients who develop hematological or renal abnormalities while receiving therapy. Cessation of these agents is of particular clinical relevance, given the loss of their impressive therapeutic potential in a range of cancers.

Material and Methods

Selection of patients

Twenty-nine patients who developed a renal syndrome following VEGF-targeted therapy underwent kidney biopsy. The clinical and laboratory studies were assessed at the time of renal biopsy and follow-up data were available for all patients (Table 1). Each patient was followed over time for the development of specific end points, including progression to severe renal failure and death.

Controls include adult patients with idiopathic glomerular diseases (MCNS, FSGS and TMA). Control renal samples (n=5) were supplied by the hospital tissue bank (platform of biological resources, Henri Mondor hospital) from patients undergoing nephrectomy for polar kidney tumor and were considered as normal by the pathologists.

Complement assays and ADAMTS13 plasma activity

Plasma concentrations of complement factor H (CFH) and factor I (CFI) were measured by enzyme-linked immunosorbent assay (ELISA), and serum levels of C4, C3, and factor B (FB), by nephelometry. Membrane cofactor protein (MCP or CD46) expression was analyzed in granulocytes using phycoerythrin (PE)–conjugated anti-CD46 antibodies (Serotec, Oxford, United Kingdom). Sequencing of CFH, CFI, and MCP genes, functional assays for ADAMTS13 plasma activity and tests for circulating antibodies to ADAMTS13 were performed as previously described.[35, 36]

Immunohistochemistry and confocal microscopy analyses

Primary antibodies used in this study included anti-VEGF, anti-HIF-1α, anti-Tie2, anti-NF-κB RelA and p50 (Santa Cruz Biotechnology, CA), anti-nephrin (Progen, Heidelberg, Germany) and anti-c-mip. Immunohistochemistry and immunofluorescence studies were

carried out in each group and specific labeling was quantified as previously described.[34] For

quantification, all glomeruli from each section, except those with significant sclerosis ($\geq$

50%), were analyzed by computer-assisted image analysis using 400x magnification. The

images were blindly analyzed by two independent investigators, as previously described.[37]

Positive staining within each glomerulous was expressed as percentage of immunostained

area over total glomerular area using image analysis software (Image J; National Institute of

Health, Bethesda, USA).[38]

Transmission Electron microscopy and immunogold labeling

Tissues were fixed with 2% glutaraldehyde in 0.1 M Na cacodylate buffer pH 7.2, for 4 hours

at room temperature and then postfixed with 1% osmium tetroxide containing 1.5% potassium

cyanoferrate, contrasted with 2% aqueous uranyl acetate, gradually dehydrated in ethanol

(30% to 100%) and embedded in Epon (Delta microscopie, Labège France). Thin sections (70

nm) were collected onto 200 mesh cooper grids, and counter stained with lead citrate, then

examined under a Zeiss EM902 electron microscope. Electron micrographs were acquired

with a charge-coupled device camera MegaView III CCD camera and analysed with ITEM

software.

For immunogold labeling, kidney biopsies (n=3) and controls (n=3) were successively fixed

with a mixture of 4% PFA/ 0.25% glutaraldehyde in 0.1 M phosphate buffer, pH 7.2 (PB) for

one hour, followed by 4% PFA, then processed for ultracryomicrotomy as described.[39] The

grids were placed on the 2% gelatine in a 37°C stove for 30 min, quenched with 50 mM

glycine in PB, blocked with 1% BSA and 10% normal goat serum (NGS), then incubated with

RelA antibody (1:30 dilution) in PB containing 1% BSA, 2% NGS for 2 hours. The grids

were washed twice, followed by incubation with goat anti-rabbit IgG coupled to 10 nm

colloidal gold particles (British Biocell International, UK). After washing, cryosections were

stained with 2% uranyl acetate, and embedded with 2% methylcellulose containing 5% uranyl

acetate. Random capillary loops were scanned by transmission electron microscopy and the

number of gold particles in podocytes and in glomerular endothelial cells were counted and

expressed as the number of gold particles per square micrometer ($Au/\mu m^2$).

Cell culture with RTKI and reverse transcription-polymerase chain reaction (RT-PCR)

Conditionally immortalized mouse podocytes have been described elsewhere.[40] Sorafenib

(BAY 439006, Enzo Life Sciences Inc.) and Sunitinib malate (Sigma Aldrich) were

dissolved in ethanol and stored at minus 20°C before use. Differentiated podocytes were

exposed to 10 mM sorafenib for 30 hours at 37°C. Then, cells were washed three times in

PBS and total RNA was prepared using RNeasy kit (Qiagen, France). Reverse transcription

was performed with Superscript II (Invitrogen, Inc, CA) and PCR amplification with

Phusion high-fidelity DNA polymerase (Finnzyme, Finland). The primers used for

amplification of mouse RelA, c-mip and RNA18S transcripts, as well as quantitative PCR

conditions are listed in Table 2.

The wild-type and RelA-deficient mouse embryonic fibroblasts (MEF) were a kind gift of

Ron Hay (University of Dundee, Dundee, UK). RelA$^{-/-}$ MEF cells were derived from the

original RelA knockout mice and have been described previously.[41] MEF cells were

synchronized in DMEM containing 2% FCS, then cultured in DMEM containing 10% FCS,

in which Sorafenib was added at a concentration of 10 μM for 24 hours.

Isolation of c-mip promoter, plasmid constructs and dual-luciferase reporter assays

We used 5'-RACE (rapid amplification of cDNA ends) to isolate the 5'UTR (untranslated

region) of c-mip using the primers indicated in Table 2. We selected oligonucleotides

spanning the 5'sequence of c-mip and the genomic DNA sequence upstream of the 5'UTR to

amplify a 1270 bp DNA fragment by PCR from human genomic DNA. The PCR product was verified by sequencing.

The human c-mip-luciferase reporter plasmid (pGl$_3$-C-mip-luc) was constructed by ligation of a 1244 bp DNA fragment containing the c-mip promoter including the transcriptional start site, into pGl$_3$-Basic (Promega) predigested with NcoI/SmaI. All constructions were verified by sequencing. The NF-kB p65/RelA and p50 expression plasmids have been described elsewhere.[42] Dual-luciferase reporter assays driven by the c-mip promoter were performed as previously reported.[43]

Chromatin immunoprecipitation (Chip) and electrophoretic mobility shift assays (EMSA)

To determine whether RelA binds *in vivo* to a specific sequence of the c-mip promoter, we performed chromatin immunoprecipitation in a podocyte cell line, using the protocol developed by Farnham PJ,[44] with minor modifications. Chromatin was sonicated on ice using six pulses of 15 sec each at amplitude 3 on a Gene Pulser (Vibra Cell model 75022). A rabbit polyclonal anti-RelA antibody (Santa Cruz Biotechnology) and rabbit IgG (control) were used to immunoprecipitate RelA-containing chromatin. The immunoprecipitated chromatin was treated with proteinase K, purified with a PCR cleanup kit (Qiagen), and concentrated by precipitation with 0.3M NaCl. The PCR primers and conditions used to amplify the murine c-mip proximal promoter and the sequences flanking the putative RelA site (CAGGGGCTGCCCC) are indicated in Table 2.

The preparation of nuclear fractions and EMSA experiments were performed as previously described.[45]

Western blot analyses and immunoprecipitations

The primary antibodies used in this study included anti- IκBα (rabbit and mouse), anti-phospho-Ser$^{32/36}$ IκBα (ref 9242, 4814 and 9246, respectively, from Upstate Cell

signaling, USA), anti-RelA and anti-phospho-Ser[276] IκBα (sc-109 and sc-101749, respectively, from Santa Cruz Biotechnology, Inc, USA), anti-Sp1 (Poly6247, BioLegend, CA), anti-Calpain (ref 208737, Calbiochem, Germany). The c-mip polyclonal antibody was produced in rabbits immunized with peptides raised against peptides located in PH and LRR domains.

Cell protein extracts from podocyte or MEF cells were prepared in lysis buffer B (150 mM NaCl, 10 mM Tris HCl pH 7.5, 2 mM DTT, 10% glycerol, 1 mM EDTA, 1% NP40, 1 mM protease inhibitors, 1 mM NaF, and 1 mM sodium orthovanadate).

Cytosolic and nuclear fractions were prepared essentially as described previously.[46] Protein concentrations were assayed using the Bio-Rad dye reagent (Bio-Rad, Richmond, CA), following the instructions provided by the manufacturer. Immunoprecipitation experiments were performed as previously described.[34]

Statistical Analysis

Data represent the mean ± SEM and were prepared using GraphPad Prism software, version 4.0. We used the Mann-Whitney test or one-way Anova to evaluate P values.

1
2
3
4
5
6
7
8
9
10
11
12
13
14
15
16
17
18
19
20
21
22
23
24
25
26
27
28
29
30
31
32
33
34
35
36
37
38
39
40
41
42
43
44
45
46
47
48
49
50
51
52
53
54
55
56
57
58
59
60

Disclosure

All the authors declared no competing interests.

References

1. Muller-Deile J, Worthmann K, Saleem M*, et al.* The balance of autocrine VEGF-A and VEGF-C determines podocyte survival. *Am J Physiol Renal Physiol* 2009; **297:** F1656-1667.

2. Guan F, Villegas G, Teichman J*, et al.* Autocrine VEGF-A system in podocytes regulates podocin and its interaction with CD2AP. *Am J Physiol Renal Physiol* 2006; **291:** F422-428.

3. Ivy SP, Wick JY, Kaufman BM. An overview of small-molecule inhibitors of VEGFR signaling. *Nat Rev Clin Oncol* 2009; **6:** 569-579.

4. Kerbel RS. Tumor angiogenesis. *N Engl J Med* 2008; **358:** 2039-2049.

5. Maharaj AS, Saint-Geniez M, Maldonado AE*, et al.* Vascular endothelial growth factor localization in the adult. *Am J Pathol* 2006; **168:** 639-648.

6. Neufeld G, Cohen T, Gengrinovitch S*, et al.* Vascular endothelial growth factor (VEGF) and its receptors. *FASEB J* 1999; **13:** 9-22.

7. Shweiki D, Itin A, Soffer D*, et al.* Vascular endothelial growth factor induced by hypoxia may mediate hypoxia-initiated angiogenesis. *Nature* 1992; **359:** 843-845.

8. Heinrich MC, Corless CL, Duensing A*, et al.* PDGFRA activating mutations in gastrointestinal stromal tumors. *Science* 2003; **299:** 708-710.

9.   Hurwitz H, Fehrenbacher L, Novotny W*, et al.* Bevacizumab plus irinotecan, fluorouracil, and leucovorin for metastatic colorectal cancer. *N Engl J Med* 2004; **350:** 2335-2342.

10.   Waller CF. Imatinib mesylate. *Recent Results Cancer Res* 2010; **184:** 3-20.

11.   Homsi J, Daud AI. Spectrum of activity and mechanism of action of VEGF/PDGF inhibitors. *Cancer Control* 2007; **14:** 285-294.

12.   Eremina V, Jefferson JA, Kowalewska J*, et al.* VEGF inhibition and renal thrombotic microangiopathy. *N Engl J Med* 2008; **358:** 1129-1136.

13.   Mathieson PW. Minimal change nephropathy and focal segmental glomerulosclerosis. *Semin Immunopathol* 2007; **29:** 415-426.

14.   Sanz AB, Sanchez-Nino MD, Ramos AM*, et al.* NF-kappaB in renal inflammation. *J Am Soc Nephrol* 2010; **21:** 1254-1262.

15.   Nowak DE, Tian B, Jamaluddin M*, et al.* RelA Ser276 phosphorylation is required for activation of a subset of NF-kappaB-dependent genes by recruiting cyclin-dependent kinase 9/cyclin T1 complexes. *Mol Cell Biol* 2008; **28:** 3623-3638.

16. Zhong H, Voll RE, Ghosh S. Phosphorylation of NF-kappa B p65 by PKA stimulates transcriptional activity by promoting a novel bivalent interaction with the coactivator CBP/p300. *Mol Cell* 1998; **1:** 661-671.

17. Arun P, Brown MS, Ehsanian R*, et al.* Nuclear NF-kappaB p65 phosphorylation at serine 276 by protein kinase A contributes to the malignant phenotype of head and neck cancer. *Clin Cancer Res* 2009; **15:** 5974-5984.

18. Izzedine H, Massard C, Spano JP*, et al.* VEGF signalling inhibition-induced proteinuria: Mechanisms, significance and management. *Eur J Cancer* 2010; **46:** 439-448.

19. Roncone D, Satoskar A, Nadasdy T*, et al.* Proteinuria in a patient receiving anti-VEGF therapy for metastatic renal cell carcinoma. *Nat Clin Pract Nephrol* 2007; **3:** 287-293.

20. Frangie C, Lefaucheur C, Medioni J*, et al.* Renal thrombotic microangiopathy caused by anti-VEGF-antibody treatment for metastatic renal-cell carcinoma. *Lancet Oncol* 2007; **8:** 177-178.

21. Izzedine H, Brocheriou I, Deray G*, et al.* Thrombotic microangiopathy and anti-VEGF agents. *Nephrol Dial Transplant* 2007; **22:** 1481-1482.

22. Bollee G, Patey N, Cazajous G*, et al.* Thrombotic microangiopathy secondary to VEGF pathway inhibition by sunitinib. *Nephrol Dial Transplant* 2009; **24:** 682-685.

23.   Henke N, Schmidt-Ullrich R, Dechend R*, et al.* Vascular endothelial cell-specific NF-kappaB suppression attenuates hypertension-induced renal damage. *Circ Res* 2007; **101:** 268-276.

24.   Guzik TJ, Harrison DG. Endothelial NF-kappaB as a mediator of kidney damage: the missing link between systemic vascular and renal disease? *Circ Res* 2007; **101:** 227-229.

25.   Takase O, Marumo T, Imai N*, et al.* NF-kappaB-dependent increase in intrarenal angiotensin II induced by proteinuria. *Kidney Int* 2005; **68:** 464-473.

26.   Yang JC, Haworth L, Sherry RM*, et al.* A randomized trial of bevacizumab, an anti-vascular endothelial growth factor antibody, for metastatic renal cancer. *N Engl J Med* 2003; **349:** 427-434.

27.   Thakker GD, Hajjar DP, Muller WA*, et al.* The role of phosphatidylinositol 3-kinase in vascular endothelial growth factor signaling. *J Biol Chem* 1999; **274:** 10002-10007.

28.   Lamalice L, Houle F, Huot J. Phosphorylation of Tyr1214 within VEGFR-2 triggers the recruitment of Nck and activation of Fyn leading to SAPK2/p38 activation and endothelial cell migration in response to VEGF. *J Biol Chem* 2006; **281:** 34009-34020.

29.   Gong C, Stoletov KV, Terman BI. VEGF treatment induces signaling pathways that regulate both actin polymerization and depolymerization. *Angiogenesis* 2004; **7:** 313-321.

30.   Veron D, Reidy KJ, Bertuccio C*, et al.* Overexpression of VEGF-A in podocytes of adult mice causes glomerular disease. *Kidney Int* 2010; **77:** 989-999.

31.   Bertuccio C, Veron D, Aggarwal PK*, et al.* Vascular Endothelial Growth Factor Receptor 2 Direct Interaction with Nephrin Links VEGF-A Signals to Actin in Kidney Podocytes. *J Biol Chem* 2011; **286:** 39933-39944.

32.   Sison K, Eremina V, Baelde H*, et al.* Glomerular structure and function require paracrine, not autocrine, VEGF-VEGFR-2 signaling. *J Am Soc Nephrol* 2010; **21:** 1691-1701.

33.   Echeverria V, Burgess S, Gamble-George J*, et al.* Sorafenib inhibits nuclear factor kappa B, decreases inducible nitric oxide synthase and cyclooxygenase-2 expression, and restores working memory in APPswe mice. *Neuroscience* 2009; **162:** 1220-1231.

34.   Zhang SY, Kamal M, Dahan K*, et al.* c-mip impairs podocyte proximal signaling and induces heavy proteinuria. *Sci Signal* 2010; **3:** ra39.

35.   Fremeaux-Bacchi V, Moulton EA, Kavanagh D*, et al.* Genetic and functional analyses of membrane cofactor protein (CD46) mutations in atypical hemolytic uremic syndrome. *J Am Soc Nephrol* 2006; **17:** 2017-2025.

36.   Veyradier A, Obert B, Houllier A*, et al.* Specific von Willebrand factor-cleaving protease in thrombotic microangiopathies: a study of 111 cases. *Blood* 2001; **98:** 1765-1772.

37.   Tesch GH, Hill PA, Wei M*, et al.* LF15-0195 prevents the induction and inhibits the progression of rat anti-GBM disease. *Kidney Int* 2001; **60:** 1354-1365.

38.   Rangan GK, Tesch GH. Quantification of renal pathology by image analysis. *Nephrology (Carlton)* 2007; **12:** 553-558.

39.   Tokuyasu KT. A technique for ultracryotomy of cell suspensions and tissues. *J Cell Biol* 1973; **57:** 551-565.

40.   Mundel P, Reiser J, Zuniga Mejia Borja A*, et al.* Rearrangements of the cytoskeleton and cell contacts induce process formation during differentiation of conditionally immortalized mouse podocyte cell lines. *Exp Cell Res* 1997; **236:** 248-258.

41.   Beg AA, Sha WC, Bronson RT*, et al.* Embryonic lethality and liver degeneration in mice lacking the RelA component of NF-kappa B. *Nature* 1995; **376:** 167-170.

42.   Thanos D, Maniatis T. The high mobility group protein HMG I(Y) is required for NF-kappa B- dependent virus induction of the human IFN-beta gene. *Cell* 1992; **71:** 777-789.

43.   Kamal M, Valanciute A, Dahan K*, et al.* C-mip interacts physically with RelA and inhibits nuclear factor kappa B activity. *Mol Immunol* 2009; **46:** 991-998.

44.   Wells J, Farnham PJ. Characterizing transcription factor binding sites using formaldehyde crosslinking and immunoprecipitation. *Methods* 2002; **26:** 48-56.

45.   Sahali D, Pawlak A, Le Gouvello S*, et al.* Transcriptional and post-transcriptional alterations of IkappaBalpha in active minimal-change nephrotic syndrome. *J Am Soc Nephrol* 2001; **12:** 1648-1658.

46.   Stein B, Rahmsdorf HJ, Steffen A*, et al.* UV-induced DNA damage is an intermediate step in UV-induced expression of human immunodeficiency virus type 1, collagenase, c-fos, and metallothionein. *Mol Cell Biol* 1989; **9:** 5169-5181.

Legends

Figure 1. Differential expression of VEGF, HIF1α, c-mip, RelA and Tie2 in glomeruli of patients with MCN/FSG-like lesions or TMA following anti-VEGF or RTKI therapies. Representative immunohistochemical analysis of VEGF (**a**), c-mip (**b**), HIF1α (**c**), RelA (**d**) and Tie-2 (**e**) in kidney biopsies of patients with renal diseases associated with anti-VEGF drugs. Note that VEGF is not detected in TMA, whereas it is little reduced in MCN-FSG-like lesions. C-mip is not detected in the glomeruli of control human kidneys (Con) or in thrombotic microangiopathy (TMA), while it is clearly visualized along the external side of the glomerular capillary loops in minimal change nephropathy (MCN). The expression of HIF-1α is highly increased in TMA glomeruli, while it is scarcely detectable in MCN/FSG-like lesions. Within TMA glomeruli, HIF-1α is mostly restricted to podocyte nuclei. The abundance of RelA is strongly increased in segmental pattern in TMA glomeruli, whereas it is decreased in MCN/FSG-like lesions, as compared to control glomeruli (Con). Tie2 was significantly upregulated after anti-VEGF or RTKI therapies. Scale bars, 20 μm. The relative abundance of these markers was measured by computer-assisted image analysis using 400x magnification and shown in (**f**). MCN/FSG-RTKI: Minimal Change nephropathy/focal and segmental glomerulosclerosis induced by RTKI. idiopathic MCNS. iFSG: idiopathic FSGS. TMAvegf: TMA induced by VEGF. iTMA: idiopathic TMA

Figure 2. Differential expression of RelA and nephrin in TMA and MCN-like lesions. Confocal microscopy analysis of nephrin (red) and RelA (green) expression in control human kidneys (Con), MCN-like lesions (MCN) and TMA biopsies. The abundance of RelA is significantly increased in TMA. RelA is colocalized with nephrin but it is also abundant inside of the capillary loops, within the TMA glomeruli. Scale bars, 10 μm.

Figure 3. Differential expression of RelA and Tie2 in TMA and MCN-like lesions. Confocal microscopy analysis of Tie2 (red) and RelA (green) expression in control glomeruli (Con), MCN-like lesions (MCN) and TMA biopsies. The abundance of RelA and Tie2 is significantly increased in TMA. Tie2 and RelA are colocalized in damaged areas within TMA glomeruli, whereas they are expressed in different cell compartments in control glomeruli. Scale bars, 10 μm.

Figure 4. Overproduction of RelA in endothelials cells in TMA. Confocal microscopy analysis of Tie2 (red) and RelA (green) expression in arterioles of control human kidneys (Con), and TMA biopsies. The abundance of RelA and Tie2 is significantly increased in TMA arterioles, which display a swelling of endothelial cells. The abundance of RelA is also increased in the pericytes of TMA arterioles. Scale bars, 10 μm. The relative abundance of RelA was assessed by quantifying the specific arteriolar fluorescence intensity in 3-D stacks of images taken by confocal microscopy and normalized to total arteriolar area. Five samples were analyzed in each condition (Con and TMA). Data represent the mean ± sem (*P<0.05, Mann Whitney test).

Figure 5. Electron microscopy analysis and distribution of RelA by immunogold labeling in TMA. (a) Representative transmission electron micrographs of the glomeruli in a patient with bevacizumab-induced TMA (right panel) and in a control kidney (left panel). **(b)** Representative immunogold labelling for Rel A (10 nm gold, indicated by the asterisks) in the glomeruli of a patient with bevacizumab-induced TMA (right panel) and in a control kidney (left panel). **(c)** Quantification of gold label for RelA in glomeruli patients with TMA (n=3)

and in control (n=3) (NS, non significant, P=0.6993; **P=0.0026; ***P=0.0006, Mann Whitney test).

Figure 6. RelA binds to c-mip promoter and prevents its transcriptional activity. (**a**) characterization of the c-mip promoter. Nucleotide sequence of the human c-mip proximal promoter region. Nucleotides are numbered to the left of the sequence with the transcription start site (TSS) indicated by the position +1. The potential CCAAT site and NF-κB responsive element (NF-κB RE) are indicated. (**b**) identification of NF-κB RE by chromatin immunoprecipitation. HEK cells were cross-linked with formaldehyde, and chromatin was immunoprecipitated with antibodies against rabbit polyclonal anti-RelA antibody or rabbit IgG (control). Immunoprecipitated DNA was analyzed by PCR using primers flanking the NF-κB RE within the human promoter (the region amplified spans from -279 to -72 relative to the transcriptional start site). (**c**) RelA binds to NF-κB recognition site on the c-mip promoter. HEK cells were transiently co-transfected with either RelA expression plasmid or its empty vector (Ev). Protein extracts (20 μg) were used for NF-κB DNA-binding assays. Nuclear extracts were incubated with the wild-type NF-κB oligonucleotide in the absence or presence of anti-RelA/p65 antibody. The specificity of NF-κB interaction was monitored by using a mutant NF-κB oligonucleotide. The quantification of NF-κB band shifts is indicated. (**d**) RelA inhibits the c-mip promoter-dependent luciferase activity. HEK cells were co-transfected with the NF-κB (RelA/p65, p50) expression plasmids and the human c-mip luciferase reporter plasmid (pGl₃-C-mip-luc). The phRL-null vector was used as an internal control for transfection. Cell extracts were prepared 24h after transfection, then luciferase activity was measured and normalized by protein content determined by using a Bradford assay. Data are presented as relative luciferase activity (firefly luciferase/the renilla

luciferase). The two-tailed t-test is used for statistical analysis (*** P<0.001, Mann Whitney test). Five independent experiments were performed.

Figure 7. Overproduction of c-mip in RelA-deficient cells. Relative expression of *RelA* and *c-mip* transcripts on total RNA from wild-type and RelA-deficient MEF. Bars represent mean value of five independent experiments with error bars indicating SEM (***P<0,001, Mann Whitney test).

Figure 8. RTKI sorafenib induces an upregulation of c-mip. (a) Left, Western-blot analysis of c-mip on total protein lysates from wild-type and RelA-deficient MEF, with or without treatment by sorafenib (10 µM). The membrane was reblotted with GAPDH antibody; left, relative abundance of c-mip corrected by GAPDH signal (from left panel). Similar results were obtained in two independent experiments. **(b)** Relative expression of *c-mip* transcript on total RNA from differentiated podocytes non-treated or treated with Sorafenib (10 µM). Bars represent mean value of three independent experiments with error bars indicating SEM (*P<0,05, Mann Whitney test). **(c)** Western-blot analysis of c-mip on total protein lysates from normal lymphocytes with (+) or without (-) treatment by sorafenib (10 µM).

Figure 9. Sorafenib inhibits RelA activation. (a) Western-blot analysis of pSer$^{32/36}$ IκBα and pSer^{276} RelA on total protein lysates from podocytes, with (+) or without (-) treatment by sorafenib (10 µM). The quantification of phosphorylated forms on total proteins is indicated in the lower panels. Bars represent mean value of three independent experiments with error bars indicated SEM (*P<0,05, one-way Anova test). **(b)** Western-blot analysis of RelA on cytoplasm and nuclear podocyte extracts of which the purity was assessed by calpain and Sp1

1
2
3
4
5
6
7
8
9
10
11
12
13
14
15
16
17
18
19
20
21
22
23
24
25
26
27
28
29
30
31
32
33
34
35
36
37
38
39
40
41
42
43
44
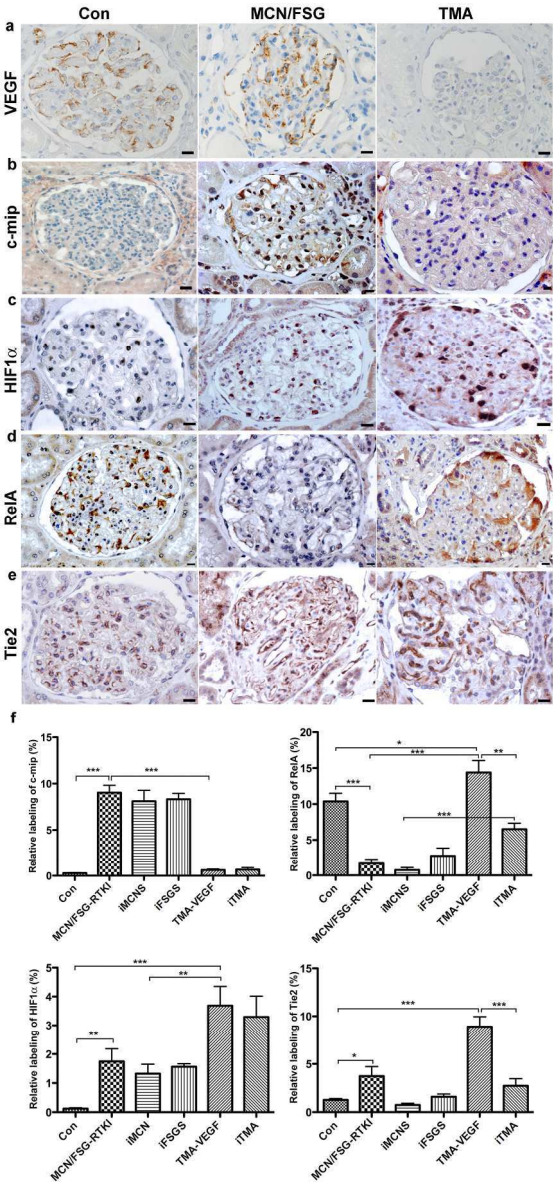45
46
47
48
49
50
51
52
53
54
55
56
57
58
59
60

bloting, respectively. Data are representative of three independent experiments. **(c)** Immunoprecipitation of RelA (rabbit antibody) from podocyte protein lysates, followed by sequential immunoblotting with mouse IκBα and RelA antibodies. **(d)** Confocal microscopy analysis of MEF cells with or without treatment by sorafenib (10 μM) for 48 hours. Similar results were obtained with podocyte cell line.

Acknowledgments

1
2
3
4
5
6
7
8
9
10
11
12
13
14
15
16
17
18
19
20
21
22
23
24
25
26
27
28
29
30
31
32
33
34
35
36
37
38
39
40
41
42
43
44
45
46
47
48
49
50
51
52
53
54
55
56
57
58
59
60

119x260mm (300 x 300 DPI)
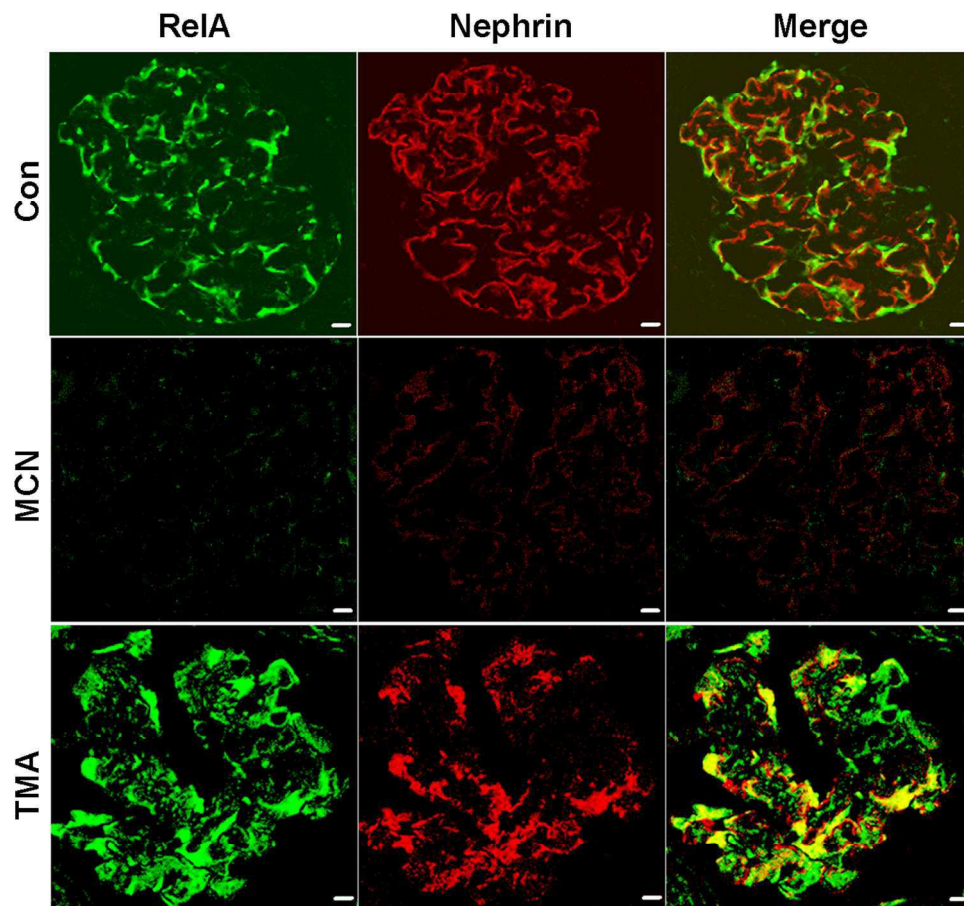
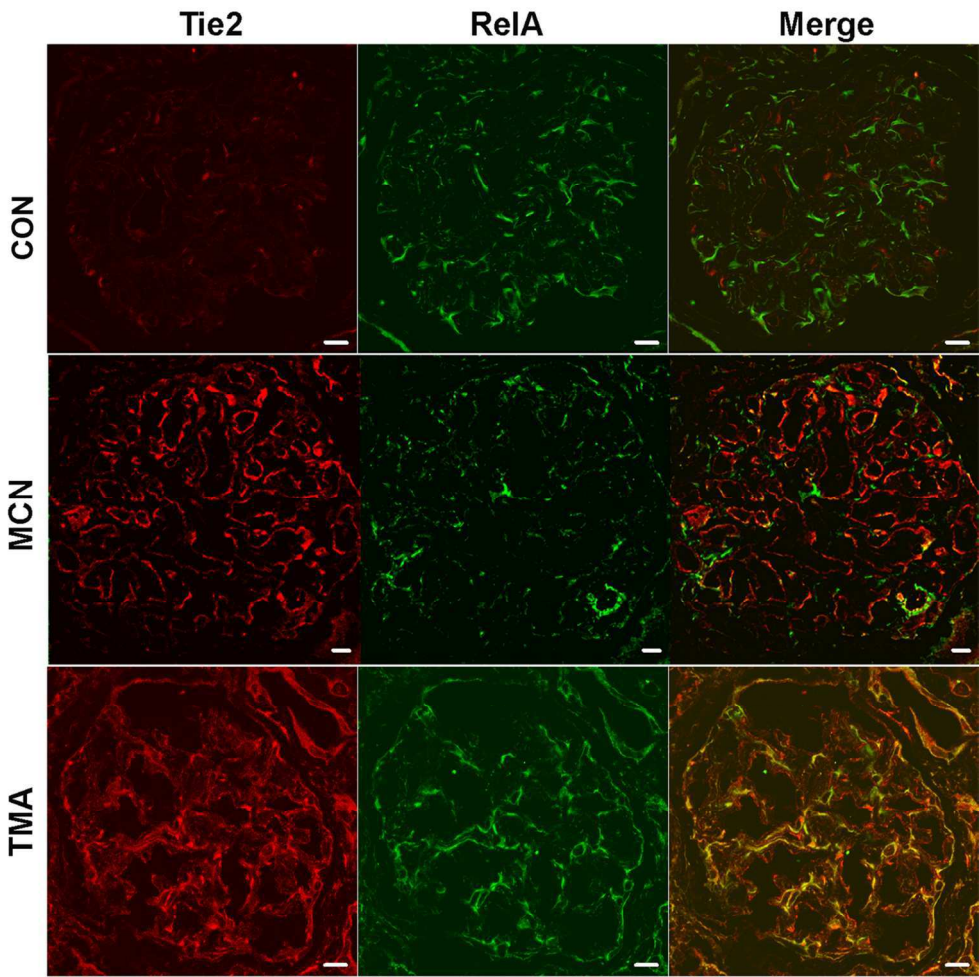119x115mm (300 x 300 DPI)

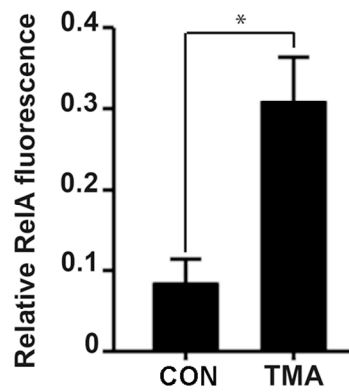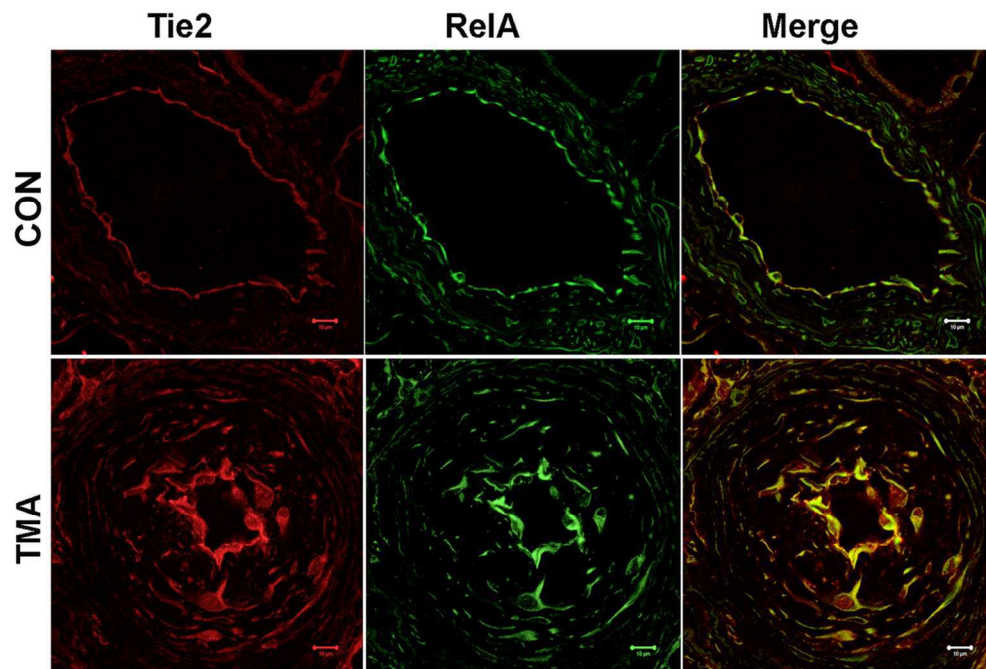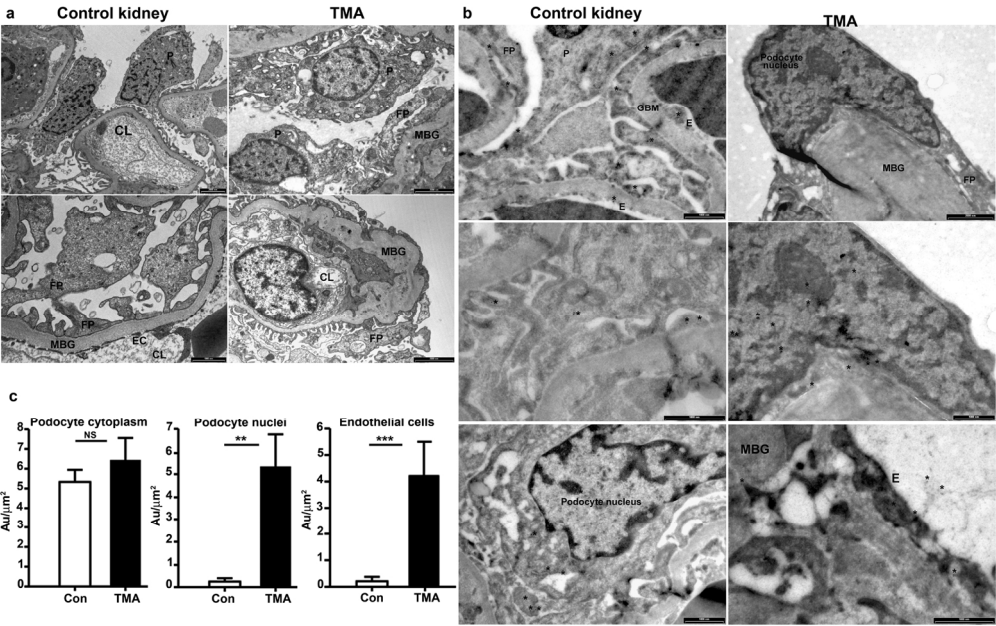**Fig. 3**

119x124mm (300 x 300 DPI)

Fig. 4

119x137mm (300 x 300 DPI)

160x99mm (300 x 300 DPI)

Fig. 6
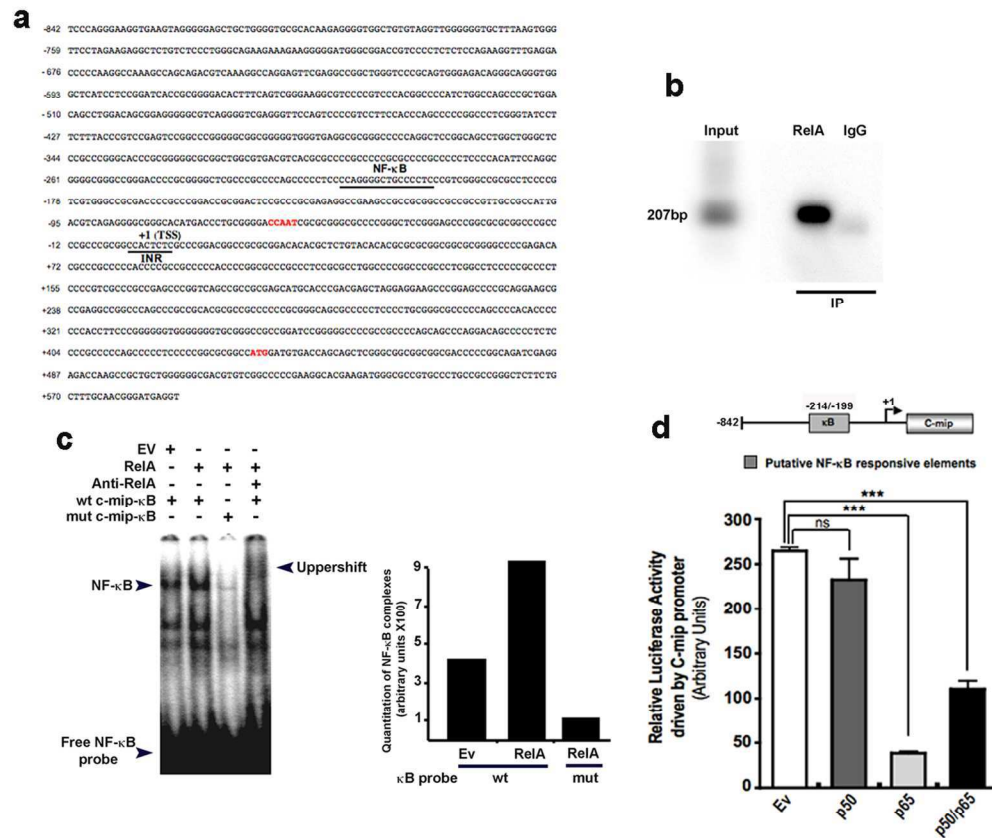
119x109mm (300 x 300 DPI)
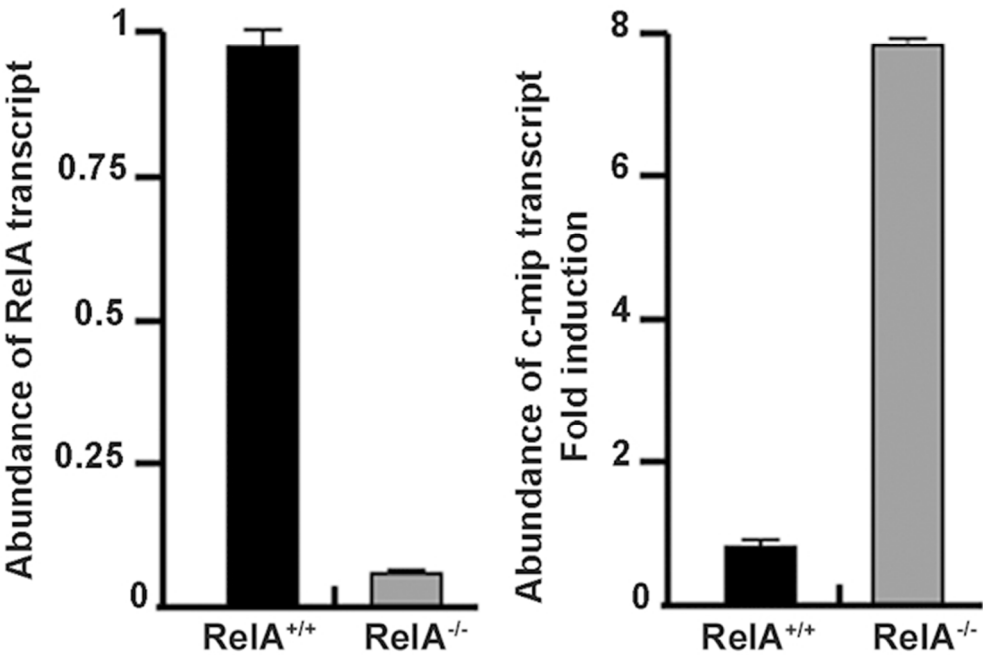
Fig. 7

60x45mm (300 x 300 DPI)

a

RelA⁻/⁻   RelA⁺/⁺

Sorafenib   -   +   -   +

c-mip

GAPDH

b

Fig. 8

c

Sorafenib   -   +   -   +

c-mip

GAPDH

86x64mm (300 x 300 DPI)

1
2
3
4
5
6
7
8
9
10
11
12
13
14
15
16
17
18
19
20
21
22
23
24
25
26
27
28
29
30
31
32
33
34
35
36
37
38
39
40
41
42
43
44
45
46
47
48
49
50
51
52
53
54
55
56
57
58
59
60
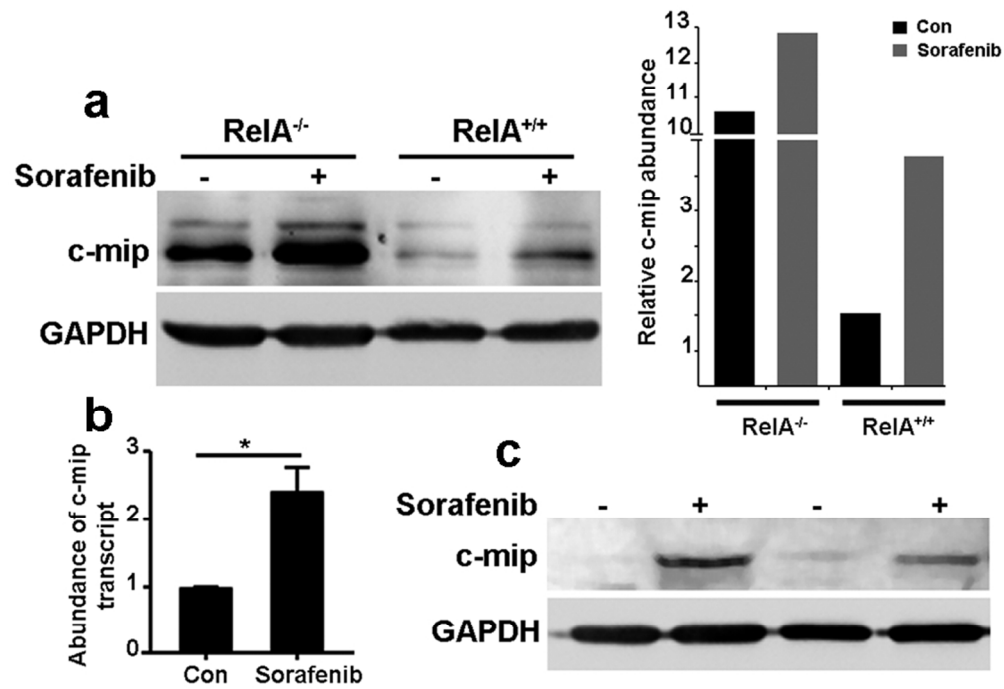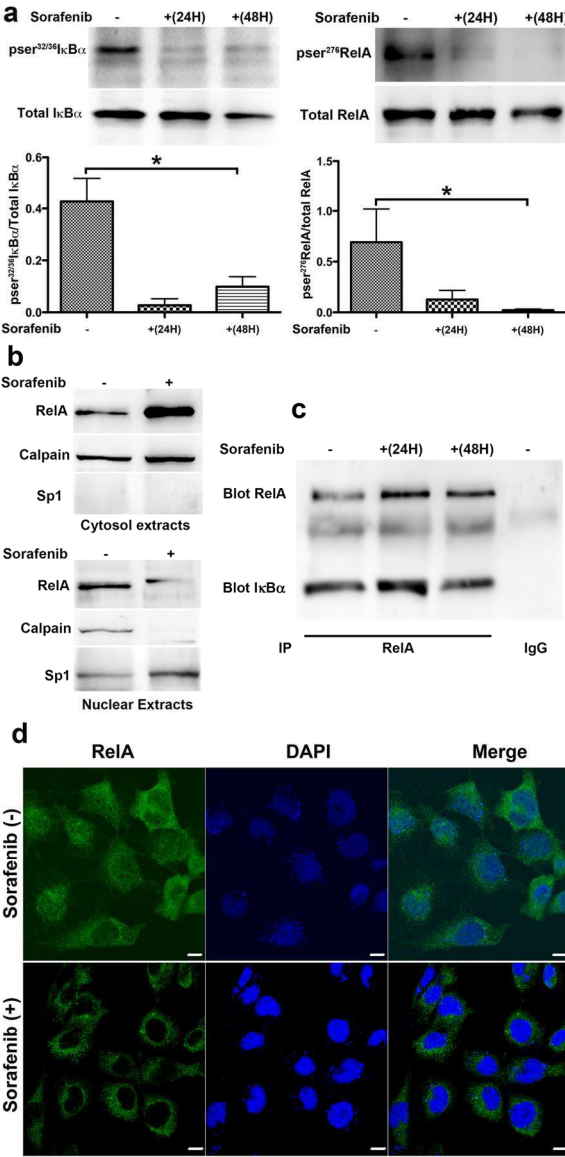
86x180mm (300 x 300 DPI)

Table 1: **Patient characteristics at baseline**

	All patients	MCN/FSG	TMA
n	29	8	13
Men	19	6	3
Age, yr, mean (range)	55.2 (20-79)	71.5 (37-79)	69.5 (20-67)
mRCC	17	7	3
Previous nephrectomy	14	6	3
Previous radiotherapy and/or IFNα use	12	5	4
Anti-VEGF agents			
Bevacizumab (cumulative dose)	9	-	6 (10-240 mg/kg)
VEGF Trap (cumulative dose)	6	-	5 (12-54 mg/kg)
Sunitinib (cumulative dose)	11	5 (50-200 mg)	2 (100 mg)
Axitinib (cumulative dose)	1	1 (40 mg)	-
Sorafenib (cumulative dose)	3	2 (800 mg)	-
Renal parameters			
SBP, mmHg, mean (range)	150.0 (110-190)	130.0 (110-180)	165.0 (120-190)
DBP, mmHg, mean (range)	95.0 (60-115)	83.0 (60-110)	100.0 (80-115)
Proteinuria, g/day, mean (range)	3.50 (0.6-19.5)	3.5 (2-5,5)	4.11 (0.6-19.5)
Edema	14	5 (62.5%)	4 (31%)
Microhematuria	12	2 (28.5%)	6 (46%)
SCr, mg/dL, mean (range)	1.26 (0.70-4.44)	0.95 (0.79-1.27)	0.86 (0.70-1.45)
aMDRD CrCl, mL/min/1.73 m2, mean (range)	76.5 (13.7-120)	76 (17-102)	75 (45-120)
Outcome			
Follow up duration	1 mo – 3 yrs	3 yrs	6 mo – 2 yrs
Alive	14	1	8
SCr, mg/dL	1.0 (0.75-2.1)	1.20	0.95 (0.75-2.1)

MCN/FSG, minimal change nephropathy/focal segmental glomerulopathy, TMA, thrombotic microangiopathy; mRCC, metastatic renal cell carcinoma; IFNα, interferon alpha; VEGF, vascular endothelial growth factor; SBP, systolic blood pressure; DBP, diastolic blood pressure; SCr, serum creatinin; aMDRD CrCl, creatinine clearance; mo, month.

1
2
3
4
5
6
7
8
9
10
11
12
13
14
15
16
17
18
19
20
21
22
23
24
25
26
27
28
29
30
31
32
33
34
35
36
37
38
39
40
41
42
43
44
45
46
47
48
49
50
51
52
53
54
55
56
57
58
59
60

Table 2. Sequence of primers and PCR conditions.

| Primers	Sequence	Accession number	Expected size	Ann Temp (°C)	PCR cycles
Mouse primers	c-mip Forward: CAGAGGTTTGCAGAAGATCCAAGA CAGGAA	XM924798	462	60	32
	Reverse: GCGGGCCAGGTCCGCATCC	NM_009045.4	420	60	30
	RelA Forward: GTGGAGATCATCGAACAGCCGAAG				
	Reverse: GCAGAGGCGCACTGCATTCAAGTC	NR_003278	151	60	16
	18S Forward: GTAACCCGTTGAACCCCATT				
	Reverse: CCATCCAATCGGTAGTAGCG				
Mouse c-mip Proximal promoter	Forward CAGACATATACTACAAGTTGGCTTC GAACGCAC		1604	65	35
	Reverse CTAAGCTGTTGTCGGCCAGCGTTAGGTG				
κB RE	RE putative site: CAGGGGCTGCCCC				
EMSA	oligonucleotide (Forward strand): 5'CCAGGGGCTGCCCCTC-3				
Chip sequence			207	58	35
	Forward: CCTCCCCACATTCCAGGCG Reverse: TCATGTGCCCGCCCCTCTG Internal probe: CGCGAGAGGCCGAAGCCGC				
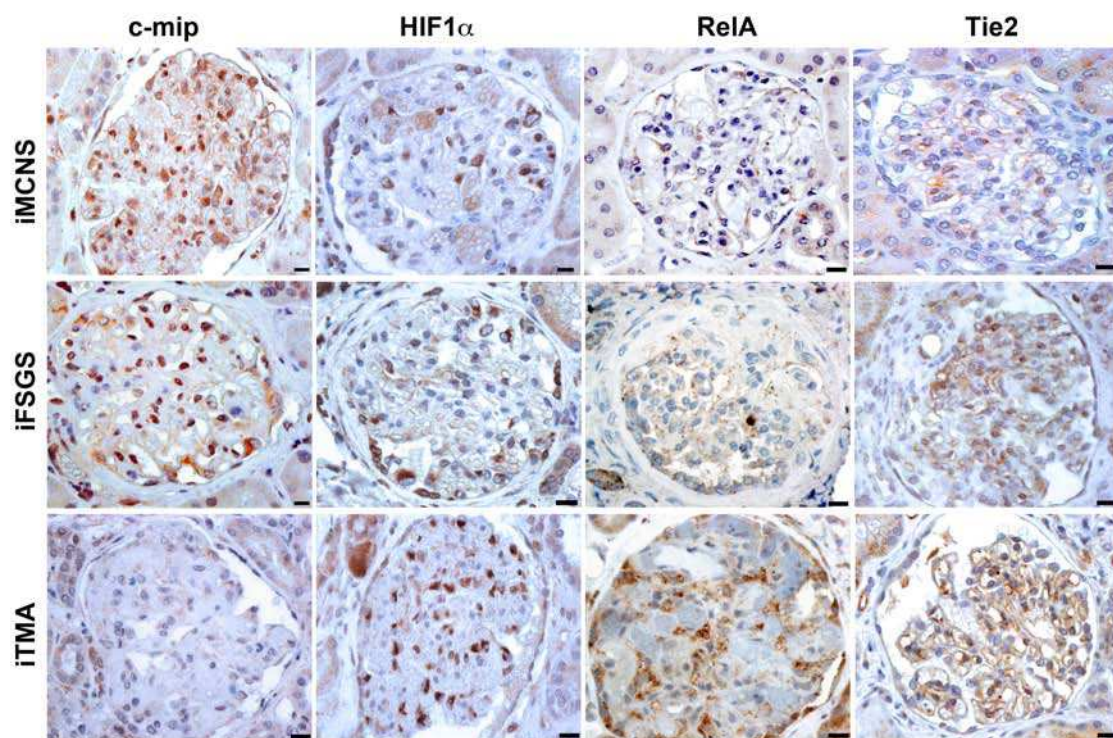
Figure S1: Representative immunohistochemical analysis of several markers in idiopathic glomerular diseases